PN:1533

Unraveling Drug Penetration of Echinocandin Antifungals at the Site of Infection in an Intra-Abdominal Abscess Model

Yanan Zhao[1]*, Brendan Prideaux[1], Yoji Nagasaki[1], Min Hee Lee[1], Pei-Yu Chen[1], Landry Blanc[1], Hsinpin Ho[1], Cornelius J. Clancy[2], Minh Hong Nguyen[2], Véronique Dartois[1], David S. Perlin[1]*

[1]Public Health Research Institute, NJMS, Rutgers University, Newark, NJ 07103
[2]Department of Medicine, Division of Infectious Diseases, University of Pittsburgh School of Medicine, Pittsburgh, PA
*Correspondence: Yanan Zhao, Ph.D. and David S. Perlin, Ph.D. Email: zhaoy1@njms.rutgers.edu; perlinds@njms.rutgers.edu

ABSTRACT

Background: Intra-abdominal candidiasis (IAC) is a prominent invasive fungal infection associated with high mortality. Prompt antifungal therapy and source control are crucial for successful treatment. Echinocandin antifungal drugs are first-line agents. Yet, their clinical effectiveness is highly variable with known potential for breakthrough resistance, and little is known about drug exposure at the site of infection. Using matrix-assisted desorption/ionization (MALDI) mass spectrometry imaging as well as standard analytical techniques, we investigated the spatial and quantitative distribution in tissue lesions for two echinocandin drugs, micafungin and CD101, in a clinically relevant IAC mouse model.

Methods: Female 6-8 week old CD1 mice weighing 18-22 g were infected intraperitoneally (IP) with 1x107 CFU of C. albicans SC5314 mixed with sterile stool matrix. Single IP doses of CD101 at 5 or 20 mg/kg (equivalent to humanized therapeutic dose) or micafungin at 5 mg/kg (therapeutic dose) were administered to mice at day 3 post-inoculation. Mice were sacrificed at just before antifungal treatment (n=1), and at 1, 3, 6, 24, and 48 h post-dose (n=3 per group per time point). Liver and kidney lesions were collected for MALDI imaging. Laser capture microdissection (LCM) followed by liquid chromatography coupled tandem mass spectrometry (LC/MS-MS) was applied to 6 and 24h samples for drug exposure measurement. In a separate experiment, mice were treated with 2 or 3 doses of micafungin (5 mg/kg), or a single dose of CD101 (20 mg/kg). Drug accumulation was analyzed at 48 and 72h post the first dose.

Results: Drug accumulation within lesions was observed with both drugs at their humanized therapeutic dose. However, micafungin, even at steady-state, failed to approach the mutant prevention concentration (MPC) (16 µg/ml) of the infecting strain. CD101 demonstrated extensive penetration into the lesions after a single dose administration and persisted in lesions at above MPC level of 29.7 µg/ml at 72h postdose.

Conclusions: These findings indicate that current echinocandin drugs may be limited by penetration at the site of infection, which have implications for clinical outcomes and emergence of resistance in patients with IAC.

INTRODUCTION

Intra-abdominal candidiasis (IAC) is one of the most common yet poorly understood types of invasive candidiasis associated with high mortality[1]. Scattered abscesses and microlesions are the predominant histopathological findings within abdominal organs from humans with IAC. Echinocandins are recommended as first-line therapy for most types of invasive candidiasis, but treatment failures occur in up to 40% of cases [2]. Limited data have suggested that echinocandin delivery to infection sites is often insufficient to achieve concentrations that eliminate Candida or suppress resistance[3], which may account for a considerable amount of treatment failures. Yet, data on the infection site pharmacokinetics (PK) of echinocandins are extremely scarce and nothing is known about penetration into tissue lesions.

Matrix-assisted laser desorption/ionization mass spectrometry imaging (MALDI-MSI) has emerged as a powerful tool to acquire spatially allocated molecular information about drug distributions in tissues[4]. Here, we took the initiative to apply this technology, as well as standard analytical techniques to investigate echinocandin drug penetration at the site of infection in a clinically relevant IAC mouse model involving *C. albicans*[5].

MATERIALS AND METHODS

Ethics statement: All animal experiment protocols were approved by Rutgers Institutional Animal Care and Use Committee.

Mouse model of intra-abdominal candidiasis and tissue sample collection: A mouse model of IAC established by Cheng et al. was used for this study (22). Female 6-8 week old CD1 mice (Charles River Laboratories) were infected intraperitoneally (IP) with $1x10^7$ CFU of *C. albicans* SC5314 mixed with sterile stool matrix as previously described. Single doses of CD101 at 20 (equivalent to humanized therapeutic dose) or 5 mg/kg, or micafungin at 5 mg/kg (therapeutic dose) were administered at day 3 post-inoculation. In a separate experiment, 3 doses of micafungin were given once daily to compare with a single dose of CD101. Mice were sacrificed at just before antifungal treatment, and at 1, 3, 6, 24, and 48 h post-dose. Livers and kidneys were explored for abscesses > 1mm in diameter, dissected, placed on a cryohistology tray, and snap-frozen in liquid nitrogen and stored at -80°C for tissue sectioning for MALDI imaging. Extra sets of 6h and 24h liver samples were also collected for absolute drug quantification and burden measurements.

MALDI-MSI analysis: MALDI-MSI analysis was performed using a MALDI LTQ Orbitrap XL mass spectrometer (Thermo Fisher Scientific, Bremen, Germany) with a resolution of 60,000 at m/z 400, full width at half maximum. For CD101, spectra were acquired in the m/z 1000-1500 range, using positive ionization with a laser energy of 25 µJ and 15 laser shots were fired at each position. Spectra for micafungin were acquired in the same m/z range under negative ionization mode with a laser energy of 10 µJ and 5 laser shots at each position. The laser step size was set at between 50-75 µm. Data visualization was performed using Thermo ImageQuest software.

Laser-capture microdissection: Necrotic lesion and surrounding tissue areas totaling 2-6 million μm^2 were dissected from between 3 and 6 serial liver or kidney biopsy tissue sections using a Leica LMD6500 system (Buffalo Grove, IL).

Drug quantitation by LC/MS-MS: LC-MS analysis was performed on a Q Exactive high resolution mass spectrometer (Thermo Fisher Scientific, Waltham, MA) coupled to a Thermo Scientific Dionex UltiMate 3000 binary system.

Statistical analysis: Absolute drug concentrations were graphed and statistically analyzed in the GraphPad software (Prism 7; GraphPad Software, Inc., San Diego, CA). Drug levels in different tissue compartment at different time points were compared by the one way analysis of variance (ANOVA) and Dunn' multiple comparison was used for the post hoc analyses. Statistical significance was defined as $P < 0.05$.

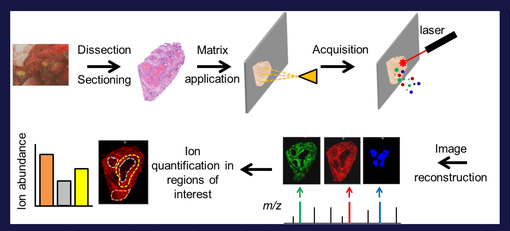

Figure 1. Overview of MALDI-mass spectrometry imaging (left) and LCM (right)

ACKNOWLEDGEMENTS

This research was supported by the NIH grant AI109025 to D.S.P. Cidara provided a deuterated form of CD101.

RESULTS

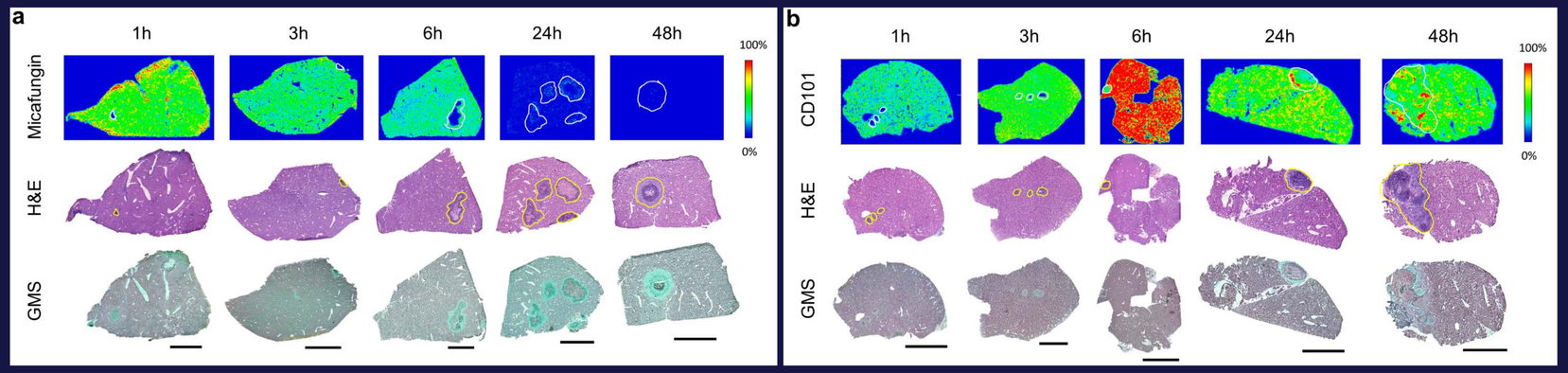

Figure 2. Drug distribution in infected liver tissues after single dose micafungin and CD101. (a) Upper row: Ion maps of micafungin in representative liver tissues collected at 1, 3, 6, 24, and 48h post a single dose of micafungin at 5 mg/kg; signal intensity color bar is fixed for micafungin, with gradually increased intensity from blue (no signal) to red (maximum signal); H&E and GMS staining of adjacent sections are shown below each set of ion maps. Outlines highlight the lesion area on each tissue section. Scale bars, 3 mm. **(b)** Upper row: Ion maps of CD101 in representative liver tissues collected at 1, 3, 6, 24, and 48h post a single dose of CD101 at 20 mg/kg; signal intensity color bar is fixed for CD101, with gradually increased intensity from blue (no signal) to red (maximum signal). Matched H&E and GMS staining results are shown in the middle and bottom rows, respectively. Scale bars, 3 mm.

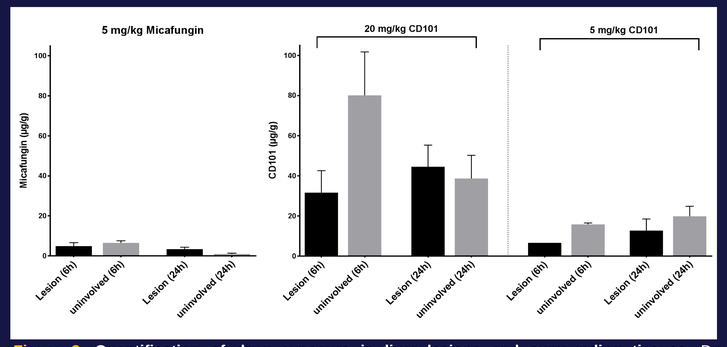

Figure 3. Quantification of drug exposure in liver lesions and surrounding tissues. Drug concentration was measured in lesions and surrounding uninvolved tissues by laser capture microdissection of liver sections collected at 6h and 24h post single dose of micafungin at 5 mg/kg or CD101 at 20 and 5 mg/kg. Error bars, mean ± s.d. of 3-5 liver pieces or distinct lesions.

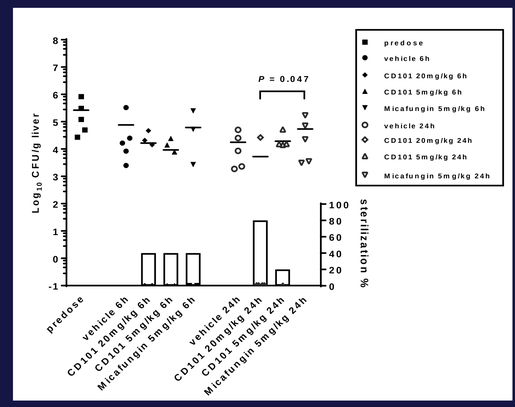

Figure 4. Liver burden comparison at 0 (predose), 6 and 24h post single dose treatment of CD101 at 20 or 5 mg/kg, micafungin at 5 mg/kg, and vehicle control. Each symbol represents liver burden of a single animal. Short lines are mean burdens determined for 5 mice in each treatment group. Symbols on the X-axis represent mice with no liver burden (sterilization). Percentage of mice with liver sterilization were plotted as bars on the right Y-axis underneath burdens of each corresponding group. Compared to micafungin, the 20 mg/kg CD101 resulted in significant burden reduction in liver at 24h postdose with a P value of 0.047, as well as percentage of sterilized animals.

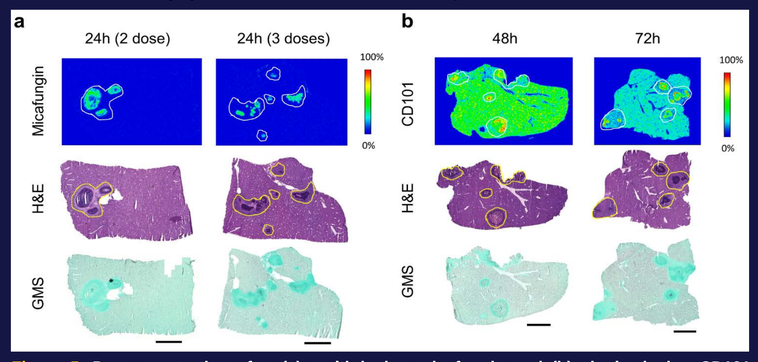

Figure 5. Drug penetration after (a) multi-dosing micafungin and (b) single dosing CD101. Micafungin is steadily being accumulated in abscesses upon 2 and 3 doses. Micafungin signal was only detected from lesion enters at steady state (after 3 doses). CD101 diffused into lesions thoroughly at 48h post single dosing, and accumulated in necrotic area of each lesion at 72h. H&E and GMS staining of adjacent sections are shown below each set of ion maps. Outlines highlight the lesion area on each tissue section. Scale bars, 3 mm.

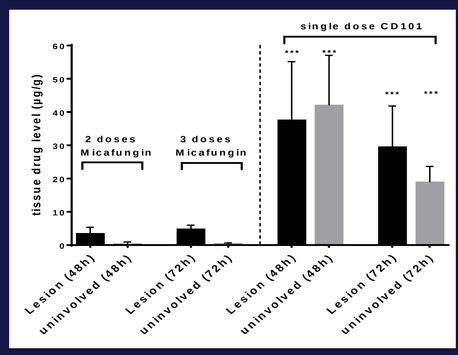

Figure 6. Drug accumulation comparison between multiple doses of micafungin (5 mg/kg) and single dose of CD101 (20 mg/kg). Absolute drug level was measured for lesions and surrounding uninvolved tissues from liver samples collected at 48h and 72h post the first dose of micafungin, and those treated with a single dose of CD101 and collected at the matched time points. Error bars, mean ± s.d. of 3-5 liver pieces or distinct lesions. *** $P < 0.001$, drug levels of CD101 were significantly higher than micafungin in corresponding sites (lesion or uninvolved tissue) at specified time point.

CONCLUSIONS

- These findings indicate that current echinocandin drugs may be limited by penetration at the site of infection, which have implications for clinical outcomes and emergence of resistance in patients with IAC.
- Drug candidate CD101 appears to overcome this penetration limitation.
- More broadly, these types of studies are relevant to a wide range of infectious and non-infectious disease pathologies that require effective drug levels for clinical response.

REFERENCES

1. Vergidis P, Clancy CJ, Shields RK, Park SY, Wildfeuer BN, Simmons RL, Nguyen MH. 2016. Intra-Abdominal Candidiasis: The Importance of Early Source Control and Antifungal Treatment. PLoS One 11:e0153247.
2. Wiederhold NP, Lewis JS, 2nd. 2007. The echinocandin micafungin: a review of the pharmacology, spectrum of activity, clinical efficacy and safety. Expert Opin Pharmacother 8:1155-1166.
3. Grau S, Luque S, Campillo N, Samso E, Rodriguez U, Garcia-Bernedo CA, Salas E, Sharma R, Hope WW, Roberts JA. 2015. Plasma and peritoneal fluid population pharmacokinetics of micafungin in post-surgical patients with severe peritonitis. J Antimicrob Chemother 70:2854-2861.
4. Prideaux B, Stoeckli M. 2012. Mass spectrometry imaging for drug distribution studies. J Proteomics 75:4999-5013.
5. Cheng S, Clancy CJ, Xu W, Schneider F, Hao B, Mitchell AP, Nguyen MH. 2013. Profiling of Candida albicans gene expression during intra-abdominal candidiasis identifies biologic processes involved in pathogenesis. J Infect Dis 208:1529-1537.